MANSOURA JOURNAL OF CHEMISTRY
Official Journal of Faculty of Science, Mansoura University, Egypt
E-mail: scimag@mans.edu.eg ISSN: 2974-4938

# Effect of βC-loaded silica nanoparticles on L-NAME -induced kidney injury in rats

***Mona Wahdan*** [a] **, *Emad Tolba*** [b] **, *Fardous F. El-Senduny*** [a] **, *Omali Y. El-khawaga*** [a] ***

[a] *Chemistry Department, Faculty of Science, Mansoura University, 35516, Mansoura, Egypt.*
*biochemmona@gmail.com*

[b] *Polymers and Pigments Department, National Research Center, 33 El Bohouth St, Dokki, 12311 Cairo, Egypt.*

***Corresponding author**: Prof. Omali Y. Elkhawaga, Email: elkhawaga70s@mans.edu.eg*
*https://orcid.org/ 0000-0002-9049-7537*

**Received:28/8/2022**
**Accepted: 17/9/2022**

**Abstract:** Renal injury (RI) is one of the most main causes of disability and mortality in several countries in the world. RI is caused when the kidneys are damaged and not functioning as they should. Renin-angiotensin-aldosterone system's (RAAS) overactivity, promotes vasoconstriction, hypertension, and renal inflammation. It is linked to the advancement of kidney disease. Herein, we assessed the ameliorative effect of treatment with beta carotene-loaded silica nanoparticles (βC-SiNPs) as a reno-protective agent on renal function and structure using $N^{\omega}$-nitro-L-arginine methyl ester (L-NAME) for induction renal injury in the male rats. Thirty-six rats were divided into six groups: Normal group (N); native beta carotene (N+βC) group; βC-loaded silica nanoparticles (N+βC-SiNPs) group; L-NAME group; L-NAME +βC group and L-NAME + βC-SiNPs group. After L-NAME and/or βC-SiNPs were administrated orally to male rats for 4 weeks, blood samples and kidneys were taken for biochemical analyses and histopathological studies. The obtained results demonstrated that the sol-gel synthesized SiNPs show spherical nanoparticles with average particles size of 290 ± 120 nm. The βc- SiNPs particles also exhibited spherical morphology with average particles size of 460 ± 160nm. βC-SiNPs have a significant reversal effect on kidney function, and markedly improved renal histopathological markers of inflammation and fibrosis.

**In conclusion**, βC-SiNPs exhibit ameliorative effects more than the native βC against L-NAME -induced RI in rats by inhibiting inflammation as it has renoprotective effect.

**keywords**:L-NAME, Silica nanoparticles, β-carotene, NOS, RAAS.

## 1.Introduction

Renal injury (RI) as a consequence of cardiovascular and metabolic diseases is becoming more common around the world. This triad of diseases is associated with a high rate of morbidity and mortality as well as significant economic burden on countries that have poor outcomes[1]. In the kidney, nitric oxide (NO) has several important functions such as renal hemodynamics regulation [2], pressure–natriuresis mediation [3], and modulation of renal sympathetic neural activity [4]. Significantly, deficient renal NO synthesis through the chronic inhibition of nitric oxide synthase by Nω-nitro-L-arginine methyl ester (L-NAME) produces progressive renal damage with systemic hypertension and interstitial macrophage infiltration, resulting in insufficient renal NO production [5]. In experimental hypertension, the balance between nitric oxide (NO) and angiotensin II (Ang II) is thought to affect renal function and renal damage progression. Ang II is known to cause uncoupling of NOS by stimulating NADPH oxidase to produce ROS that affects NO's bioavailability, preventing NOS from producing NO [6]. Furthermore, L-NAME appears to exacerbate the renal injury, most likely due to a decrease in NO generation. Renin-angiotensin-aldosterone system's (RAAS) overactivity is induced by ROS

resulting in the disruption of key cellular processes such as high blood pressure, oxidative stress, fibrosis, hypertrophy, and inflammation. Consequently, these diseases result in deadly renal and cardiovascular complications [7].

The kidney is considered as an endocrine gland with an internal structure that revealed two different regions, the cortex, a marginally placed, and pale outer part and the medulla an inner, darker section, are both visible [8]. The renal pelvis, the renal artery and vein, the lymphatics, and a nerve plexus flow through the medial or concave surface of the kidney, known as the hilus, and enter the sinus of the kidney. The lateral surface has a significant curvature, smooth and curved [9]. Histologically, a capsule made of collagen fibers and connective tissue surrounds the kidney cortex and can be easily detached. Nephrons, functional renal units that filter the blood of waste materials including uric acid, water, and other ions, are part of the cortex. A cortex is consisting of nephrons that are a functional units of kidney and filtered the blood from waste such as uric acid, water and other ions. The medulla is split into 8 to 18 striated conical masses, the renal pyramids, and is situated internally to the cortex toward the hilus of the kidney. Each pyramid's base is expanded in the direction of the renal pelvis to create a papilla, which opens in the renal pelvis and continues into the ureter [10, 11].

In the last few decades, several studies demonstrated that the use of natural products as an alternative for the treatment of many disorders has increased with high specificity and selectivity for treatment with low side effects [12]. Carotenoids, one of the natural products, as phytochemicals that are highly efficient in preventing and lowering the symptoms of numerous illnesses, including cancer, Alzheimer's disease, cerebral ischemia, obesity-related diabetes, hypertension, and ophthalmic disorders [13]. Among carotenes, beta carotene (βC) has an essential role as a therapeutic drug (natural bioactive pharmaceutical molecule) due to its provitamin A activity and high antioxidant capacity than other carotenoids. It was used as a standard model for a long period of time to study the relationship between oxidative stress and chronic diseases. βC has low bio-accessibility, poor absorption, and bioavailability based on the poor hydrophilicity, stability, and sensitivity towards light, temperature, and pH [14]. According to the literature reports, appling nanoparticles in drug delivery may provide advantages over more conventional delivery techniques. For instance, it has been discovered that utilizing nanocarriers of small optimum size can deliver loaded medications more precisely and selectively to target tissues [15]. The ability of drug nanocarriers with the right size range to pass through small blood capillaries and avoid phagocytosis allows for a prolonged period of circulation for the nanoparticles. Additionally, the regulated release of medications is made possible by the use of nanocarriers in drug delivery, which also minimize any potential negative side effects [16]. As a biocompatible nanocarrier, silica nanoparticles (SiNPs) are considered as having special qualities such as versatility, stability, large surface area, high drug loading efficiency, potential functionalization with other materials and high hydrophilic surface [17] . So, nanoincorporation into a proper silica nanoparticle with βC to improve its efficacy and bioavailability as a renoprotective and anti-inflammatory agent in hypertensive rats. Thus, the current study aimed to evaluate the impact of βC-loaded onto silica nanoparticles (βC-SiNPs) on the biochemical and histopathological changes associated with renal injury using the L-NAME induced rat model in comparison with βC.

## 2.Materials and methods

### 2.1.Chemicals

Silica nanospheres precursors (tetraethyl orthosilicate TEOS), β- carotene (βC) and Nω-nitro- L-arginine methyl ester (L-NAME) were purchased from Sigma-Aldrich Company, USA. Sodium bicarbonate ($NaHCO_3$), ammonium hydroxide solution ($NH_4OH$, 28%) and ethanol (96%) were provided by supplied by Carlo Erba Reagents. All the reagents and other chemicals were of high analytical grade.

### 2.1.Preparation of silica nanoparticles (SiNPs)/ βC-SiNPs

Silica nanospheres were prepared by hydrolysis of TEOS in the presence of sodium bicarbonate salt ($NaHCO_3$) and ammonium hydroxide solution ($NH_4OH$) [18]. In brief,

sodium bicarbonate was dissolved in a mixture of water and ammonium hydroxide (5:1 v/v). The silica precursor solution was prepared by dissolving 4 ml tetraethyl orthosilicate (TEOS) in methanol (50 mL). Afterward, the TEOS/methanol mixture was slowly added to the sodium bicarbonate solution and kept under stirring at 30° C for 4h. The silica gel was collected by centrifugation at 4500 xg for 10 min and washed three times with water and twice with methanol. The obtained gel was dired at 40° C overnight. The preparation of βC-SiNPs was carried out using the same procedure, as described above, however a definite amount of βC powder was added to silica precursor solution (TEOS/methanol mixture).

**2.1.Characterizations of (βC-SiNPs)**

**2.1.1.Morphological Observation**

The particle morphology and size of the prepared nanoparticles were examined using field emission scanning electron microscopy (FE-SEM) (JSM 6360LV, JEOL/Noran).

**2.1.Animal ethics**

A total of 36 adult male Wister rats were randomly divided into six equal groups. Animals were purchased from VACSERA, Egypt. Rats were acclimatized for 1 week in the animal-care facility, Zoology Department, Faculty of Science, Mansoura University, Egypt. All animals were housed in an environment with 12-hour light-12-hour dark cycles, Rats were placed under specific pathogen-free conditions (SPF) and were fed with standard food and drinking water before starting the study. Animal experimental procedures for this study were approved by the Animal Ethics Committee of the Faculty of Science, Mansoura University, Egypt (Code number Sci-Ch-p-2021-135).

**2.1.Induction of renal injury in animal model by L-NAME**

Rats were fasted for 12 hr before oral administration with a freshly prepared solution of Nitro-L-arginine methyl ester hydrochloride (L-NAME) (40 mg L-NAME /kg body weight/day/2 weeks) [19] , then the treatment with native β-Carotene (10 mg βC/kg body weight/day/2 weeks) [20] and nano formulated β-Carotene for 2 weeks after induction of L-NAME dose. The rats were randomly allocated and similarly grouped into six groups of six rats each:

**A-Normal group (N)**: Control rats, received 0.5 ml corn oil using an intragastric tube.

**B-Normal + β-Carotene (N + βC)**: β-Carotene -treated rats, received (10 mg βC/kg b.wt/day/2 weeks) dissolved in corn oil.

**C- Normal + βC-loaded silica nanoparticles (N + βC-SiNPs)**: βC-SiNPs treated control rats, received an equivalent dose (10 mg βC/kg b. wt/day/2 weeks), orally with vehicle saline solution.

**D- L-NAME** group (**L-NAME)**: L-NAME -treated rats, received (40 mg L-NAME /kg b. wt /day/2weeks) orally with vehicle saline solution.

**E-L-NAME+ β-Carotene (L-NAME+ βC)**: L-NAME was administrated first, then rats treated with β-Carotene, received (10 mg βC/kg b.wt/day/2weeks) dissolved in corn oil.

**F**: **L-NAME+ βC-loaded silica nanoparticles (L-NAME+ βC-SiNPs)**: L-NAME was administrated first, then rats treated with βC-SiNPs, received an equivalent dose to (10 mg βC/kg b.wt/day/2 weeks), orally with vehicle saline solution. After completion of the experimental protocol, all animals have fasted overnight.

**2.2.Blood and tissue sampling**

Decapitation was used to sacrifice the animals. After blood collection, samples were left to clot for 30 min. In order to analyze several biochemical indicators, serum samples were collected by centrifugation at 3000 x g for 10 min and stored at -20° C. The kidney was dissected right away, cleaned in ice-cold saline, blotted dry, and stored for testing various biochemical markers

**2.1.Biochemical measurements**

Serum creatinine [21] and urea [22] were measured spectrophotometrically using commercial kits (Biodiagnostic, Egypt).

**2.1.Histological examination**

Fixed tissues were dehydrated using ethyl alcohol concentrations of 70, 80, 90, and 95% for 30 min each, followed by 20 min of clearing in xylene before being soaked with melted paraplast. For the histochemical analysis of interstitial fibrosis and tubular atrophy, 5 µm thickness section slides were stained with hematoxylin and eosin (H&E) [23], the cortex and medulla of the sections were evaluated for

glomerular, tubular, vascular, and interstitial inflammation. Masson trichrome (MT) which displays cellular components in red and collagen-rich areas in blue, and periodic acid-Schiff (PAS) stain to reveal glomerulosclerosis, to demonstrate polysaccharides, neutral mucopolysaccharides, and glycoproteins in epithelial tubular membranes. After being exposed to periodic acid for five minutes, the portions were cleaned with distilled water. The sections were then counter-stained with hematoxylin for 30 sec after treated with Schiff's reagent for 15 min [24]. After that, all specimens were mounted for light microscopic analysis.

**2.1.Statistical Analysis**

All data were introduced as mean ± SEM., SPSS version 22 (SPSS, Chicago, IL, USA) was applied to obtain the statistical analysis. One-way analysis of variance (ANOVA) test was utilized to study the statistical significance of the parameters among groups with a significance value P-value < 0.05.

**2.Results and Discussion**

**3.1 Preparation of silica nanoparticles (SiNPs)/ βC-SiNPs**

Figure 1 shows the preparation of (SiNPs) and βc- SiNPs before and after drying at 40$^{o}$ C. Formation of the white colloidal form of SiNPs upon hydrolysis process (sol) and then into a colloidal network (gel) after condensation/polymerization reaction to form either individual separated particles or continuous polymer structures. Preparation of colloidal form βc- SiNPs with orang colored combination between beta carotene and silica nanoparticles.

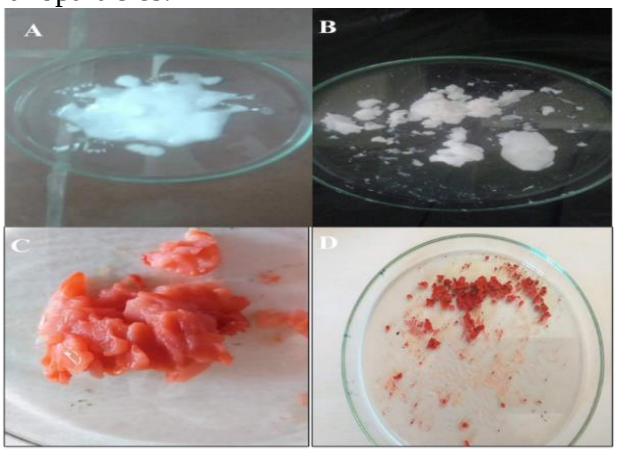


**Fig 1:** Preparation of (SiNPs) and βc-SiNPs:(A)/(B) SiNPs before/after drying. (C)/(D) βc- SiNPs before/after drying.

**3.2 Characterization of SiNP using SEM**

Silica nanoparticles were prepared by sol-gel process based on Stöber route to prepare nanosize SiNPs *via* hydrolysis and condensation of TEOS in water/methanol mixture containing $NH_4OH$ and $NaHCO_3$ [25]. The morphology of the prepared SiNPs was controlled by the amount of $NaHCO_3$ salt which acts as a templet for silica structure (Figure 2). The obtained SiNPs were spherical with average particles size of 290 ± 120nm (Figure 2A, B). However, the βc-SiNPs particles also exhibited spherical morphology. The incorporation of βc results in an increase of average particles size (460±160nm) (Figure 2C, D).

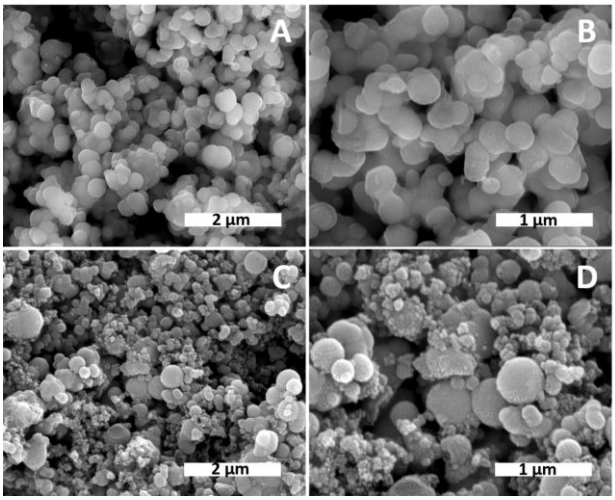


**Fig 2:** SEM images of the prepared silica nanoparticles (A, B) SiNPs and (C, D) βc-SiNPs

**3.3 Biochemical parameters**

The target of the current study was to compare the biological action of the new stable beta carotene nanoformulation to that of its native form in order to assess its potential usage as a promising renoprotective agent. Furthermore, the study used a rat model of L-NAME-induced renal damage to provide the first comparative evaluation of βC and βC-SiNPs as potent antioxidant agents. As hypertensive nephropathy (HN) is a condition of renal damage as chronic high blood pressure (BP) [26]. The cardiorenal cycle is controlled by vital regulators such as the RAAS, sympathetic nervous system, and NO**.** So, blockade of nitric oxide (NO) production with L-NAME, an L-arginine analog, as an exogenous inhibitor of nitric oxide synthase (NOS) results in cardiac and renal dysfunction.

The kidney function in L-NAME-treated rats was characterized by a significant elevation in the serum creatinine (Figure 3A) and urea (Figure 3B) compared to the control group as ($P < 0.001$). The kidney function exhibited an elevation in creatinine that is endogenously produced and released into the body and its clearance is a measure of the glomerular filtration rate, urea level elevation as being a major nitrogen-containing metabolic compound necessary for protein metabolism indicates hypertension-induced renal damage which is in agreement with previous studies [27]. Treatment with βC reduced the effect of L-NAME on the renal function compared to the corresponding values of L-NAME treated group while the significant decrease in serum creatinine and urea was attained upon treatment with βC-SiNPs. Similar data were reported by Gallo *et. al.* [28], while these results were disapproved by Li *et. al.*, [29]. Our study showed a significant improvement with βC-SiNPs more than that exhibited in the native form.

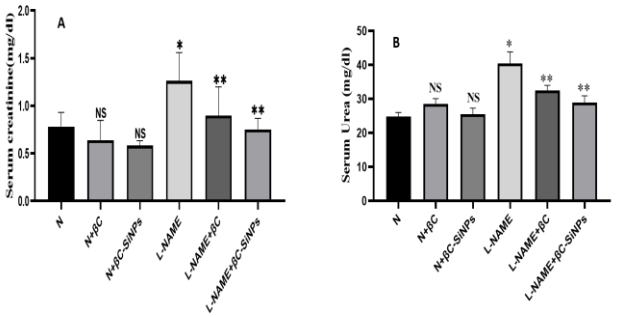


**Fig 3:** The effects of L-NAME and/or βC-SiNPs on kidney function tests, the level of Creatinine (mg/dl) (A), Urea (mg/dl) (B) in the serum of rats in different groups. Each chart showed mean ± SEM (n=6). The differences among all groups have been assessed by One-Way ANOVA with ($P < 0.05$) is considered significant.

### 3.3.Histopathological examination

Histopathological effects of L-NAME and/or βC-SiNPs rats' kidneys were investigated (figures 4, 5, and 7). The healthy group showed normal kidney while L-NAME treated rats revealed severe histological alterations with renal tubular degeneration, resulting in clear kidney injury. However, rats treated with βC-SiNPs exhibited less remarkable kidney damage based on the subsequent observations;

**A- Haematoxylin and Eosin**

In control-treated rats, normal morphology with no pathological alterations observed, i.e., normal appearance of the renal corpuscle (RC), glomerulus (G) surrounded by Bowman's capsule noticed within mentioned groups (Figures 4A, 4B and 4C). However, L-NAME treated rats showed a significant morphological change with increasing the signs of lesions, that demonstrated widening of the capsular space (crossed arrow), glomerular atrophy (arrow), interstitial congestion, clear necrosis in epithelial cells within renal tubules, in addition to some pyknotic nuclei (tailed arrows) and inflammatory cells (thick arrow) (Figure 4D). Significant recovery of the majority of the renal architecture, and many irregularly shaped proximal convoluted tubules (PT) except the occurrence of a little enlargement in the renal space of the glomerular capsules were observed in the L-NAME treated with βC group and βC-SiNPs group (Figures 4E, 4F). The L-NAME-induced renal damage is characterized by structural changes in the kidneys with decrease of kidney function. Histological findings also show ~~a~~ significant morphological changes, including an increase in lesions, glomerular atrophy, interstitial congestion, and clear necrosis in epithelial cells within renal tubules in L-NAME treated rats, compared to a normotensive group, and reversal was observed with βC-SiNPs treatment.

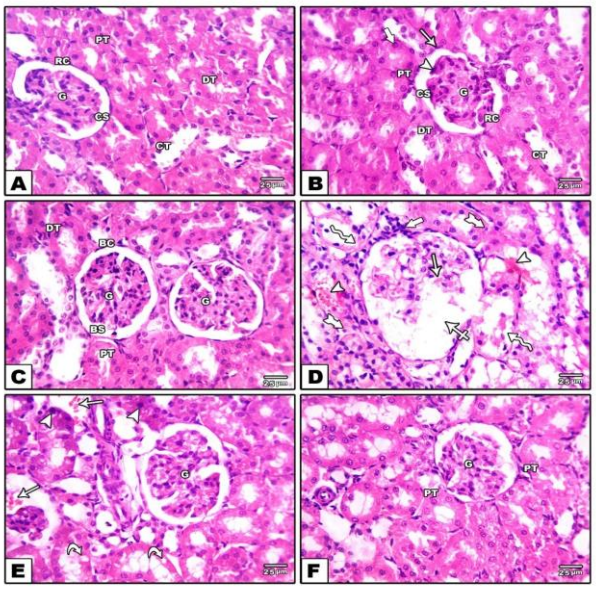


**Fig 4:** Representative photomicrograph of thick H & E-stained paraffin section from renal cortex of rats**,** Renal cortex of control group (**A**)

and **(B)** normal rat treated βC (10 mg /kg/day/2weeks) showing normal structure of the renal corpuscle **(**RC**),** glomerulus (G) surrounded by Bowman's capsule which has two layers, outer parietal simple squamous epithelial layer **(arrow)** and inner visceral layer formed of podocytes (arrow head**),** capsular space (CS) is noticed between the two layers. Proximal convoluted tubules (PT) have rounded vesicular nuclei (**thick arrow**)., distal convoluted tubules (DT) and collecting tubules (CT) are present in normal shape. **(C)** Normal rat treated βC-loaded silica nanoparticles (βC-SiNPs) showing glomerular capillaries (G) surrounded by Bowman's capsule, which is lined by simple squamous epithelium (BC).**(D)** L-NAME treated rat showing showing shrunken glomerular capillaries (arrow) and widening of the capsular space (crossed arrow). The proximal convoluted tubules have wide lumen with loss of their apical brush border (zigzag arrows). pyknotic nuclei (tailed arrows). Inflammatory cells (thick arrow). **(E)** L-NAME-treated rats with βC displaying almost normal showing apparently normal glomerular capillaries (G) and minimal vacuolation in proximal tubular lining cells (curved arrows) with small darkly stained nuclei (arrow heads) and haemorrhage area are be seen between tubules (arrows)and **(F)** L-NAME-treated rats with (βC-SiNPs) with the normal histological structure of the glomerulus (G), multiple proximal convoluted tubules (PCT). All photos X 400.

**B- Masson trichrome stain**

In L-NAME treated rats, Masson trichome (MT) stain showed the rapid spread of the mild interstitial fibrosis within examined renal tissues (Figure 5D). However, fibrosis was barely noticed in rats treated with a βC-SiNPs group (Figure 5F) confirming the ameliorative effect of βC-SiNPs on renal tissues. In addition, fibrosis was scarcely observed in βC treated group (Figure 5E). Indeed, control and/or βC-SiNPs -treated groups showed little sensitivity to the presence of fibers (Figures 5A, 5B and 5C). These histological results of collagen deposition were scored as a percentage in Figure 6. Since renal fibrosis is one of the major complications associated with the development of kidney damage, *Col-IV* is a crucial component of the glomerular basement membrane and is significantly increased in those with renal fibrosis [30]. Masson trichome stain was used to assess the dynamic status which is an alternation of the renal collagen network. As collagen synthesis and degradation coexist in the kidney and their balance determines renal collagen volume, in the study under discussion, L-NAME treatment resulted in a noticeably increased collagen deposition with mononuclear inflammatory cell aggregation in the interstitial tissue. However, significant inhibition was observed with βC-SiNPs treatment, i.e., reasonable to assume that the ameliorative effect of βC-SiNPs on L-NAME-induced renal damage and reduction of renal collagen volume caused by its antioxidant action and inhibition of RAAS through inhibition of ACE [31, 32].

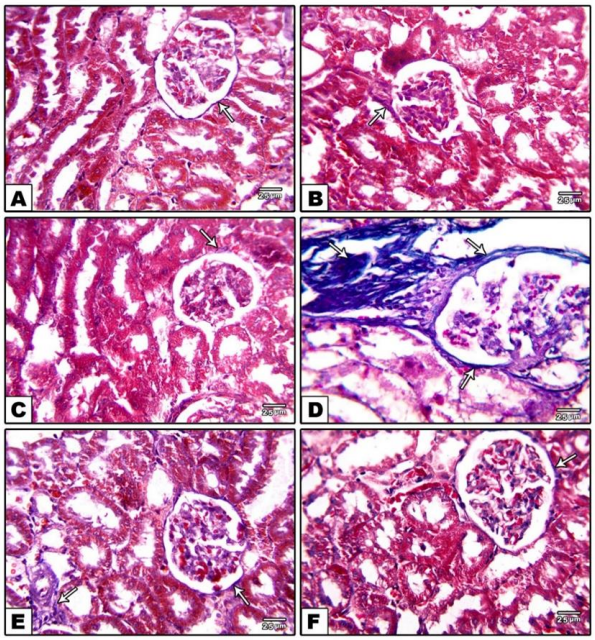


**Fig 5:** Representative photomicrograph of Masson trichrome stain from renal cortex of rats, Masson Trichrome (MT) stain demonstrated collagen deposition control group (**A**) showing an almost negative reaction, **(B)**, **(C)** normal rat treated βC and normal rat treated with (βC-SiNPs)respectively, exhibited a weak fibrous tissue reaction around renal corpuscle (arrow). (**D)** L-NAME treated rat showing massive MT reaction among convoluted tubules, around renal corpuscle (arrows) **(E)** L-NAME-treated rats with βC mild fibrous tissue deposition in some area (arrows). **(F)** L-NAME-treated rats with (βC-SiNPs) showing minimal fibrous deposition around renal corpuscle (arrow). (arrows). All photos X 400.

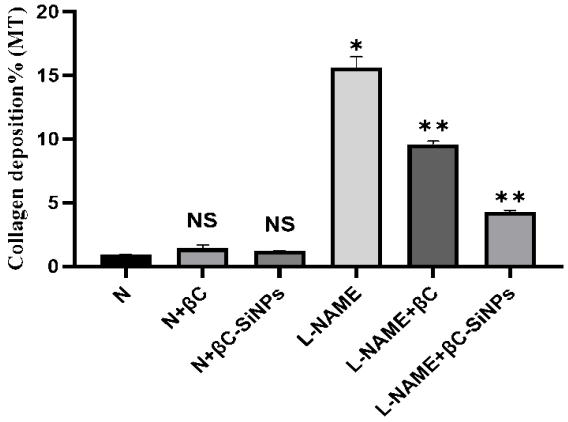


**Fig 6:** Representative percentage of collagen deposition of Masson's trichrome stain from the kidney of rats.

**C- Periodic acid-Schiff (PAS) stain**

PAS stain was used for the assessment of the extent of glycogen in renal tissues within the different groups. There were evident improvement signs within rats treated with βC/ βC-SiNPs (Figures 7E and 7F) compared to L-NAME treated ones that exhibited widespread of mesangial mass and marked glycogen depletion. Control and/or βC-SiNPs treated groups displayed the normal intact glycogen characteristic within samples (Figures 7A, 7B and 7C). L-NAME treated rat displayed depletion magenta color renal corpuscle and appears inside cells (arrow heads) (Figure 7D), this results in agreement with Abbas *et. Al.* [33].

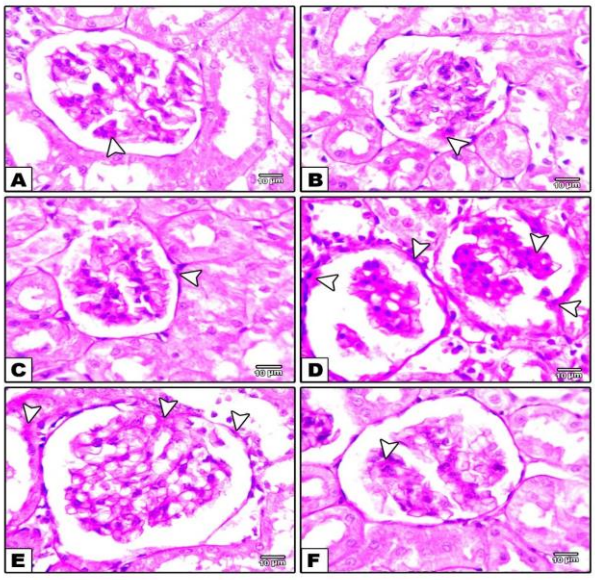


**Fig 7:** Representative photomicrograph PAS-stained from kidney of rats. PAS stain showing renal cortex tissue demonstrated negative glycogen accumulation (arrow head). control group (**A**), **(B)** normal rat treated βC respectively and normal rat treated with (βC-SiNPs) **(C)** weak glycogen accumulation around renal corpuscle (arrow head). (**D)** L-NAME treated rat displayed slight depletion in magenta color renal corpuscle and appears inside cells (arrow heads). **(E)** L-NAME-treated rats with βC showing mild glycogen accumulation in renal tissue (arrow heads). **(F)** L-NAME-treated rats with (βC-SiNPs) exhibited showing mild glycogen accumulation (arrow heads). All photos X 400.

## 4 Conclusion

The current study is designed out to explore the formulation of βC-SiNPs using stober method with modification as the addition of sodium bicarbonate, as a templet for silica structure precipitation. The SEM characterization showed that the sol-gel synthesized SiNPs are spherical nanoparticles with average particles size of 290 ± 120nm. However, the βc- SiNPs particles exhibited spherical morphology with average particles size of 460 ± 160nm. Indeed, βC-SiNPs ameliorate the determined effect of the L-NAME-treated induced renal injury model in male rats by decreasing elevation of the renal function parameters due to its renoprotective effect. Also, βC-SiNPs reduced the increased fibrosis rate caused by L-NAME in the kidney as elevation of collagen deposition. Moreover, βC-SiNPs has a potent effect in improving the histological structure of renal tissues. These findings identify that βC-SiNPs is considered as a promising nano formulated form of βC to offer a new candidate to prevent or palliate renal disease more than its native form.

## 5 References

1 Kellum, J.A., et al., (2021) Acute kidney injury. Nat Rev Dis Primers,. **7(1):** p. 52.

2 Majid, D.S. and L.G. NavarNitric (2001)., oxide in the control of renal hemodynamics and excretory function. *Am J Hypertens*, **14**(6 Pt 2): p. 74s-82s.

3 Majid, D.S., A. Williams, and L.G. Navar, (1993). Inhibition of nitric oxide synthesis attenuates pressure-induced natriuretic responses in anesthetized dogs. *Am J Physiol*, **264(**1 Pt 2): p. F79-87.

4 Eppel, G.A., et al., ( 2003). Nitric oxide

in responses of regional kidney perfusion to renal nerve stimulation and renal ischaemia. Pflugers Arch, **447(2):** p. 205-13.
5 Ikeda, H., et al., (2009). Spironolactone suppresses inflammation and prevents L-NAME-induced renal injury in rats. Kidney Int, **75(2)**: p. 147-55.
6 Cave, A.C., et al., (2006). NADPH oxidases in cardiovascular health and disease. Antioxid Redox Signal, **8(5-6):** p. 691-728.
7 Patel, S., et al., ( 2017)Renin-angiotensin-aldosterone (RAAS): The ubiquitous system for homeostasis and pathologies. Biomed Pharmacother. **94**: p. 317-325.
8 Samuelson, D.J.L., (2007) missouri, Textbook of Veterinary Histology, Saunders Elsevier, St.
9 Al-Kelaby, W.J., et al., (2018). Histological and biochemical evaluation of the efficiency of rabbit kidney after partial or radical nephrectomy **18**: p. 2033-2042.
10 Bacha Jr, W.J. and L.M. Bacha, .( 2012) Color atlas of veterinary histology: John Wiley & Sons.
11 Eurell, J.A. and B.L. Frappier, (2013): Dellmann's textbook of veterinary histology. John Wiley & Sons.
12 Shaffie, N.M., et al., (2010). Effect of caraway, coriander and fennel on the structure of kidney and islets of Langerhan in alloxan-induced diabetic rats: Histological and histochemical study. *Journal of American Science*, **6(9):** p. 405-418.
13 Bhatt, T. and K. Patel, ,( 2020). Carotenoids: Potent to Prevent Diseases Review. Nat Prod Bioprospect**10(3):** p. 109-117.
14 Reboul, E., (2013). Absorption of vitamin A and carotenoids by the enterocyte: focus on transport proteins. Nutrients, **5(9):** p. 3563-81.
15 Mathur, M. and G. Vyas, (2013). Role of nanoparticles for production of smart herbal drug– An overview
16 Wang, A.Z., R. Langer, and O.C. Farokhzad, (2012). Nanoparticle delivery of cancer drugs. Annu Rev Med, **63**: p. 185-98.
17 Argyo, C., et al., (2014). Multifunctional mesoporous silica nanoparticles as a universal platform for drug delivery. *J Chemistry of materials*, **26(1):** p. 435-451.
18 Stöber, W., et al., (1968). Controlled growth of monodisperse silica spheres in the micron size range. **26(1)**: p. 62-69.
19 Lerman, L.O., et al., (2019). Animal Models of Hypertension: A Scientific Statement From the American Heart Association. Hypertension, **73(6)**: p. e87-e120.
20 Kini, D., et al., ( 2019). Potential protective role of beta carotene on cadmium induced brain and kidney damage. **10(9)**: p. 509-512.
21 Schirmeister, J., H. Willmann, and H. Kiefer, , (1964). [plasma creatinine as rough indicator of renal function]. Dtsch Med Wochenschr**89**: p. 1018-23.
22 Fawcett, J.K. and J.E. Scott, (1960) A rapid and precise method for the determination of urea. *J Clin Pathol*,. **13(2):** p. 156-9.
23 Fanelli, C., et al., ( 2017) Gender Differences in the Progression of Experimental Chronic Kidney Disease Induced by Chronic Nitric Oxide Inhibition. Biomed Res Int 2017: p. 2159739.
24 Ozkurt, M., et al., (2018). Erythropoietin Protects the Kidney by Regulating the Effect of TNF-α in L-NAME-Induced Hypertensive Rats. Kidney Blood Press Res, **43(3)**: p. 807-819.
25 Mizrahi, D.M.J.M.T.P., (2017.) Facile one-step synthesis of silica micro-and nanotubes and their functionalization. **4(7):** p. 7083-7092.
26 Kalra, J., et al., (2020). Up-regulation of PKR pathway contributes to L-NAME induced hypertension and renal damage. Heliyon, **6(11):** p. e05463.
27 Selim, M.S., H.A. Awad, and D.A.A. Labib, (2020). Potential Effects of Empagliflozin in L-NAME-Induced Hypertensive Nephropathy in Albino Rats. *Biomedical Pharmacology Journal*, **13(1)**: p. 399-416.
28 Gallo, L.A., et al., (2016). Once daily administration of the SGLT2 inhibitor, empagliflozin, attenuates markers of renal

fibrosis without improving albuminuria in diabetic db/db mice. Sci Rep, 6: p. 26428.
29 Li, L., et al., (2018). Effect of a SGLT2 inhibitor on the systemic and intrarenal renin-angiotensin system in subtotally nephrectomized rats. *J Pharmacol Sci*, **137(2):** p. 220-223
30 Miner, J.H., (2012) The glomerular basement membrane. Exp Cell Res,**.** **318(9):** p. 973-8.
31 Ahmed, M.M., et al., (2016). Potential effect of sitagliptin on experimentally induced hypertensive nephropathy in Albino rats. World J Med Sci**13 (2):** p. 93-102.
32 Abdel-Rahman, R.F., et al., (2017). Antihypertensive Effects of Roselle-Olive Combination in L-NAME-Induced Hypertensive Rats. Oxid Med Cell Longev, 2017: p. 9460653.
33 Abbas, R., et al., (2020). Syzygium Aromatium Ameliorates Oxidative Stress and Fibrosis in Adenine-Induced Chronic Kidney Disease in Rates. **14(3):** p. 322-338.